

LQER: Low-Rank Quantization Error Reconstruction for LLMs

Cheng Zhang*, Jianyi Cheng†, George A. Constantinides*, Yiren Zhao*

*Department of Electrical and Electronic Engineering

Imperial College London
London, United Kingdom

†Department of Computer Science and Technology

University of Cambridge
Cambridge, United Kingdom

Email: cheng.zhang122@imperial.ac.uk, jianyi.cheng@cl.cam.ac.uk, g.constantinides@imperial.ac.uk, a.zhao@imperial.ac.uk

Abstract—Post-training quantization of Large Language Models (LLMs) is challenging. In this work, we introduce Low-rank Quantization Error Reduction (LQER), which combines quantization and low-rank approximation to recover the model capability. LQER leverages an activation-induced scale matrix to drive the singular value distribution of quantization error towards a desirable distribution, which enables nearly-lossless W4A8 quantization on various LLMs and downstream tasks without the need for knowledge distillation, grid search, or gradient-base iterative optimization. Unlike existing methods, the computation pattern of LQER eliminates the need for specialized Scatter and Gather processes to collect high-precision weights from irregular memory locations. Our W4A8 LLMs achieve near-lossless performance on six popular downstream tasks, while using $1.36\times$ fewer hardware resources than the leading state-of-the-art method. We will open-source our framework once the paper is accepted.

I. INTRODUCTION

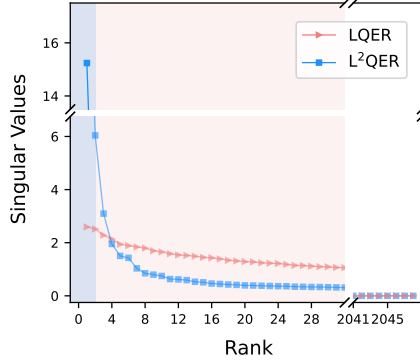
Large Language Models (LLMs) have exhibited impressive capability on various natural language processing (NLP) tasks [1]. However, the substantial model size and its associated computation costs demand considerable energy and hardware resources. For instance, deploying BLOOM-176B [2] requires 16 NVIDIA A100 GPUs and consumes more than 2000 Watts of total power [3]. Meanwhile, empirical evidence suggests that only models with a sufficiently large parameter count begin to show *emergent capabilities* [4], thereby motivates the construction of even larger models. Quantization then emerges as a promising technique to enhance the accessibility of LLMs by reducing the model size and simplifying inference computation.

Low-precision Post-Training Quantization (PTQ) of LLMs has recently become an attractive solution for reducing computational and memory cost [5]. However, it remains challenging due to the fact that 1) no further weight training is allowed and 2) the presence of magnitude outliers in model weights and activations. PTQ is a technique that quantizes a pre-trained LLM directly, without additional training, as fine-tuning LLMs usually requires substantial resources. Many researchers have observed that the main building block of LLMs, the transformer layer, produces magnitude outliers in weights and activations [6, 7, 8]. A simple fixed-point quantization then

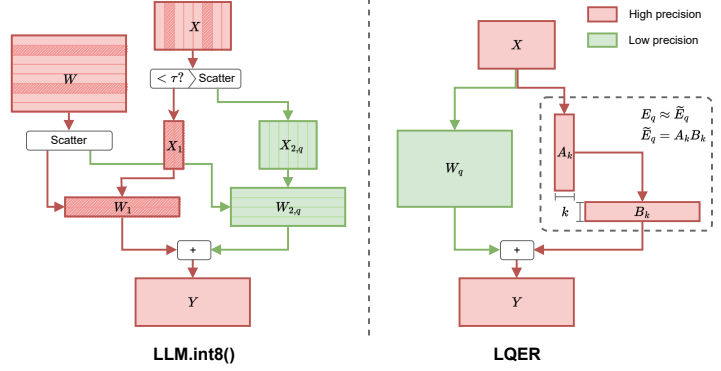
either suffers from considerable clipping or overflow error or from considerable rounding error, depending on the choice of scaling. In both cases, the quantization error propagates and accumulates through the LLMs, leading to substantial task accuracy degradation. To overcome this challenge, recent LLM PTQ methods investigate the statistical properties of LLMs and propose various fine-grained solutions to accommodate [9, 10], mitigate [11, 12], or eliminate [13, 14] these numerical outliers.

However, fine-grained treatments to numerical outliers usually come with a high optimization and/or hardware cost. The optimization cost mainly stems from iterative optimization. For example, OmniQuant [15] takes 7.3 hours to quantize a LLaMA-30B model with 20 iterations on a single NVIDIA A100 GPU [16]. The popular weight-only quantization setup, such as GPTQ [10] and AWQ [17], dequantizes 4-bit weights to FP16 at runtime, which actually impedes inference on models larger than 7B [18]. Concurrently, many existing quantization frameworks select values from irregular positions for high-precision computation, while maintaining other values in low-precision formats [19, 20]. For instance, `LLM.int8()` [9] selects activation outliers to compute in half-precision floating-point, while casting the rest to integers. In this work, we propose a simple and efficient LLM PTQ framework that avoids iterative optimization and irregular computation patterns.

Optimizing weight quantization can be considered as a process of minimizing the quantization error $E_q = W - W_q$, where W_q is the quantized weights. We are firstly interested in a novel *inference framework formulation* termed *LQER*. LQER approximates the real value of W through two components ($W = \tilde{E}_q + W_q$): a high-precision yet low-rank matrix \tilde{E}_q that approximates E_q but with $\text{rank}(\tilde{E}_q) \ll \text{rank}(W)$; and a low-precision yet high-rank matrix W_q as shown in Figure 1b. Both components are inexpensive to compute and thus work together to reduce the overall computational complexity. Crucially, the high-precision, low-rank component \tilde{E}_q establishes a regular computation pattern that eliminates need of having the Scatter and Gather operations to fetch and store values from irregular memory locations like `LLM.int8()`



(a) Singular value distributions of quantization error



(b) `LLM.int8()` v.s. LQER

Fig. 1: Motivation and computation pattern of LQER. (a) We apply SVD to the quantization error $E_q = W - W_q$ for a 3-bit fixed-point quantized weight in OPT-1.3B, and plot their singular values distributions. Distributions are normalized to have the same Frobenius norm for a fair comparison¹. Curves with a more asymptotic trend suggest better suitability for low-rank approximation. L^2QER displays a much steeper distribution with a smaller number of dominating singular values. (b) LQER approximates a trained weight W with two high-precision yet low-rank matrices A_k and B_k , and a low-precision yet high-rank matrix W_q . Both components are inexpensive to compute. This establishes a regular computation pattern that eliminates the need for irregular memory access like the Scatter and Gather operations in `LLM.int8()`.

(Figure 1b).

In this study, we explore optimizations for W_q using both the integer format and the recently proposed MX number formats [24]. Additionally, our work emphasizes the design of \tilde{E}_q . Theoretically, assuming the trained weights to be independent and identically distributed (i.i.d.), and given a sufficiently high chosen precision, E_q can be approximated as a random matrix formed by the round-off error. The Marchenko–Pastur distribution suggests that *there exhibits an asymptotic behavior for the distribution of singular values of large random matrices* [25]. We then show the actual singular value distributions of E_q in Figure 1a from a linear layer in OPT-1.3B [26] (labeled as LQER), showcasing a similar phenomenon to what the *Marchenko–Pastur law* has suggested. Further motivated by the fact that matrices with only a few large singular values like E_q can be effectively approximated by low-rank matrices. We propose to left-multiply E_q by a diagonal matrix S , derived from activation magnitudes, that pushes the singular values of E_q toward an even more desirable distribution (labeled as L^2QER in Figure 1a). The singular values of SE_q decay more rapidly than E_q , with the large singular values of SE_q concentrates in the first few components, as illustrated in Figure 1a¹. This observation then further motivates our LLM Post-Training Quantization (PTQ) method, *Left-multiply LQER* (L^2QER), designed to recover the performance loss caused by quantization. We make the following contributions in this work:

- We introduce a novel quantized LLM inference framework termed **Low-rank Quantization Error Reduction** (LQER)

¹To make a fair comparison, we normalize E_q before SVD by multiplying E_q with a scalar α such that the scaled αE_q has the same Frobenius norm as SE_q .

which combines quantization and low-rank approximation. Unlike existing methods that require gathering values from irregular memory locations, LQER boasts a blocked and regular computation pattern and employs a unified number format for both memory and computation.

- We then propose L^2QER , a straightforward but efficient quantization method on top of LQER. L^2QER does not need any expensive knowledge distillation, hyper-parameter search, or other forms of iterative optimization. We showcase L^2QER 's competitiveness with current state-of-the-art methods. L^2QER quantizes both weights and activations, it extends pushes the limit to W4A6, matching the perplexity of OmniQuant (W6A6) on WikiText. Compared to weight-only (w -only) quantization methods, our approach outperforms AWQ (W4A16) and maintains quantization activations staying at 8-bit (W4A8).

II. RELATED WORK

A. Post-Training Quantization of LLMs

Post training quantization of LLMs is a challenging task due to presence of numerical outliers. Existing methods can be broadly categorized into two setups: weight-only (w -only) and weight-activation ($w\&a$) quantizations. Recent works within these two setups are summarized in Table I.

a) *Weight-only quantization*: Weight-only quantization usually partitions the trained weight matrix W into groups, with the i -th group being quantized using a scale factor s_i :

$$(W_q, \mathbf{s}) = \mathbf{q}(W) \quad (1)$$

where W_q is the quantized weight matrix, \mathbf{s} is a vector of scale factors, and $\mathbf{q}(\cdot)$ denotes quantization function. During

TABLE I: A summary of recent LLM PTQ methods. Weight-only (w -only) and weight-activation ($w&a$) quantizations are two popular setups. w -only quantization generally dequantize values ($\text{dq}(\cdot)$) back to FP16 before the weight-activation matrix multiplication at inference time. $w&a$ quantization performs low-precision multiplication ($X_q W_q$) at inference-time but requires finding an invertible matrix S to decrease the magnitude range of activations (detail explained in Section II-A). We shortlist the recent works that belong to the two setups in the last column. * indicates the common precision of W_q and X_q that achieves almost lossless performance on downstream tasks.

Q setup	WxAy*	Quantization function	Inference-time	Methods
w -only	W4	$(W_q, \mathbf{s}) = \text{q}(W)$	$\tilde{Y} = X \text{dq}(W_q, \mathbf{s})$	GPTQ [10], AWQ [17], Z-fold [21], QuiP [22], FlexRound [20], LRQ [23]
$w&a$	W8A8	$(X_q, \mathbf{s}_t) = \text{q}(XS)$ $(W_q, \mathbf{s}_c) = \text{q}(S^{-1}W)$	$\tilde{Y}_{i,j} = \mathbf{s}_{t,i} \mathbf{s}_{c,j} (X_{q,i,:} \cdot X_{q,:,j})$ $(Y_{q,i,:}, \mathbf{s}'_{t,i}) = \text{q}([\tilde{Y}_{i,1}, \tilde{Y}_{i,2}, \dots])$	SmoothQuant [11], OS+[13], AQAS [12], OmniQuant [15]

inference, the low-precision weights W_q is dequantized back to FP16 before the weight-activation matrix multiply:

$$\tilde{Y} = X \text{dq}(W_q, \mathbf{s}) \quad (2)$$

Here X is the FP16 input, and $\text{dq}(\cdot)$ is the dequantization function, and \tilde{Y} is the output. The runtime dequantization cost is negligible in memory-bound scenarios, *e.g.*, small models at small batch sizes. *This cost escalates with model sizes, and eventually impedes inference in compute-bound scenarios* [18].

GPTQ [10] and AWQ [17] are two representative w -only quantization methods. GPTQ employs second-order information to iteratively round grouped weights and correct the quantization error in the remaining groups. AWQ protects salient weights induced by activations using per-channel scaling. Recent advancements in w -only setup include Z-Fold [21] and QuiP [22], following GPTQ to correct quantization error. FlexRound [20], and LRQ [23] follow AWQ to study finer-grained weight scaling.

b) Weight-activation quantization: $w&a$ quantization utilizes an invertible matrix S to reduce the magnitude range of activations before quantization:

$$(X_q, \mathbf{s}_t) = \text{q}(XS) \quad (3)$$

where \mathbf{s}_t is a vector a per-token scalars. S^{-1} is fused into the weights of the preceding layer before quantization:

$$(W_q, \mathbf{s}_c) = \text{q}(S^{-1}W) \quad (4)$$

where \mathbf{s}_c is a vector of per-channel scalars. At inference time, the inner product in the activation weight matrix multiplication consists of an inner product of two fixed-point vectors and an FP16 multiplication between the token scalar and channel scalar (“Inference-time” entry in Table I). Then each row of output activation matrix is quantized back to the input format. This style of quantization avoids the extra dequantization cost in w -only setup, but achieving a precision lower than W8A8 while maintaining nearly-lossless model capability proves challenging. Existing $w&a$ quantization methods lower than 8-bit precision usually suffer from an average downstream task accuracy drop larger than 1% [15, 27].

SmoothQuant [11] pioneered fusion of an invertible scale matrix into its preceding layer. Outlier Suppression+ [13] further introduces a bias matrix to Equation (4) to shift the mean of activations towards zero and update the layer bias accordingly. Recent works following this line of research include AQAS [12], and OmniQuant [15].

Another unique $w&a$ quantization method, `LLM.int8()` decomposes the FP16 matrix multiplication into a 8-bit fixed-point and an FP16 sub-matrix multiplication using activation thresholds. Despite achieving the closest model capability to FP16, the thresholding, Scatter and Gather operations of `LLM.int8()` are expensive in large models. Similar to `LLM.int8()`, SpQR [19] and EasyQuant [8] are recent works that retains salient weights in FP16 at finer granularity while quantizing the rest to low-precision.

In this work, we propose a fundamentally different PTQ framework that approximates the real value of weight through two components ($W = \tilde{E}_q + W_q$), and demonstrate how this formation helps us to achieve almost lossless PTQ in the $w&a$ quantization setup with a W4A8 configuration.

B. The MXINT Arithmetic

Block floating point is a family of number formats that represents a vector of numbers using a shared exponent or exponent bias. Various block floating point formats have been explored for efficient training or inference in the past few years [28, 29, 30, 31]. One notable representative is MXINT, introduced for hardware-efficient post training quantization [28, 32], this number format has recently been standardized by AMD, Arm, Intel, Meta, Microsoft, NVIDIA, and Qualcomm, for next-generation AI facilities [33].

Figure 2 illustrates an example of an MXINT vector sharing a 4-bit exponent across four 4-bit mantissas. MXINT excels in hardware efficiency compared to floating point, as the inner product of two MXINT vectors can be computed as a inner product of two fixed-point numbers plus an exponent addition. Meanwhile, the shared exponent provides a larger dynamic range than fixed point numbers. Recent works indicate that this extended dynamic range fits the activation outliers well

MXINT (4e3m)
4-bit shared exponent across 4 elements, 1-bit sign, 3-bit mantissa

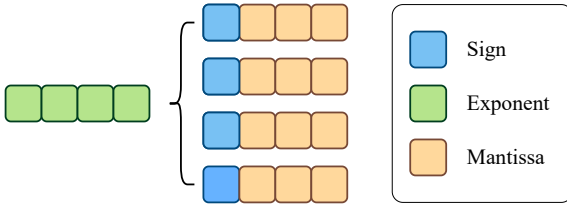


Fig. 2: MXINT number format [24]. MXINT places a shared exponent across a group of fixed-point numbers. MXINT is more hardware efficient than floating point for its simplified vector inner product, and provides a large dynamic range compared to fixed-point numbers. MXINT has been standardized recently for next generation AI hardware systems [33].

in LLM PTQ tasks [34, 24]. In this work, We adopt MXINT as the default number format while the idea can be applied to other formats.

C. Low-Rank Adapters for Fine-Tuning

Low-rank adapter (LoRA) [35] is a parameter efficient fine-tuning method for saving GPU memory. LoRA freezes the pretrained weight W , and only updates two low-rank weight matrices L_1 and L_2 during fine-tuning. Based on LoRA, qLoRA [36] keeps the quantized pretrained weights in memory and only double-dequantizes² it in the forward pass to further reduce fine-tuning memory footprints:

$$Y^{\text{BF16}} = X^{\text{BF16}} \text{ddq}(c_1^{\text{FP32}}, c_2^{\text{k-bit}}, W^{\text{NF4}}) + X^{\text{BF16}} L_1^{\text{BF16}} L_2^{\text{BF16}} \quad (5)$$

The advantage of LoRA-based methods is that the fine-tuned model can be deployed without extra cost as the low-rank matrices are fused into the pretrained weights after fine-tuning. For qLoRA, the fusion can be expressed as:

$$W_{\text{new}}^{\text{BF16}} = \text{ddq}(c_1^{\text{FP32}}, c_2^{\text{k-bit}}, W^{\text{NF4}}) + L_1^{\text{BF16}} L_2^{\text{BF16}} \quad (6)$$

LoftQ [37] initializes L_1 and L_2 with the Singular Value Decomposition (SVD) of quantization errors to achieve a faster fine-tuning convergence than qLoRA.

To our knowledge, LoftQ is the closest work to ours. However, our LQER framework is fundamentally different from the above as it is a PTQ method that does not target fine-tuning. The core idea of LQER is that shaping the singular value distribution of quantization error approximator (\tilde{E}_q) enables a nearly-lossless inference pass quantization. LoftQ fuses the low-rank matrices back to original FP32 weights when deployed, however, the low-rank matrices in LQER remains separate from the quantized weight matrix W_q ; this

²Double-dequantize means the dequantization scales the 4-bit weight matrix twice using c_1^{FP32} and $c_2^{\text{k-bit}}$

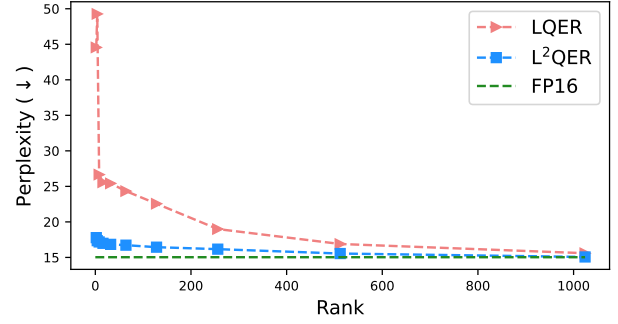


Fig. 3: Perplexity (\downarrow) vs rank. We apply W3A8 LQER and L^2 QER to OPT-1.3B and plot the resultant perplexity. Considering the embedding dimension is 2048, LQER requires a fairly large $k \approx 600$ to reach a perplexity close to FP16. In comparison, a small $k \approx 64$ is enough for L^2 QER. Comparison of perplexity (\downarrow) and quantization error reconstruction between LQER and L^2 QER.

allows the matrix multiplications for the low-precision high-rank weight matrix (W_q) and the low-rank high-precision matrices to happen in parallel at inference time.

III. METHOD

We aim to approximate the multiplication by a large dense weight matrix W in a low-cost way. This low cost can be achieved through low-precision quantization or low-rank approximation. Quantization simplifies the multiplication arithmetic, while low-rank approximation reduces the overall number of computations. We judiciously combine the two: approximate W as a dense low-precision matrix W_q and then correct the error induced using a high-precision low-rank correction term as illustrated in Figure 1b.

A. LQER: Approximated E_q using SVD

Our idea is to reconstruct the quantization error matrix E_q through SVD-based low rank approximation. When a quantization is applied to a trained FP32/FP16 weight matrix $W \in \mathbb{R}^{m \times n}$, the resulting quantization error matrix E_q is:

$$E_q = W - W_q \quad (7)$$

where $W_q = q(W)$ is the quantized weight matrix, and $q(\cdot)$ represents the quantization function. A straightforward way to reconstruct the error is to use SVD-based low-rank approximation:

$$E_q = U \Sigma V^T \approx U_k \Sigma_k V_k^T \quad (8)$$

where $U \in \mathbb{R}^{m \times m}$ and $V \in \mathbb{R}^{n \times n}$ are orthogonal matrices, $\Sigma \in \mathbb{R}^{m \times n}$ is a diagonal matrix of singular values. $U_k \in \mathbb{R}^{m \times k}$, $V_k \in \mathbb{R}^{n \times k}$ and $\Sigma_k \in \mathbb{R}^{k \times k}$ are the sub-matrices of U , V and Σ corresponding to the largest k singular values.

If two high-precision matrices $A_k = U_k$ and $B_k = \Sigma_k V_k^T$ are assigned to approximate E_q , *i.e.*, $A_k B_k \approx E_q$, the linear layer can be approximated as:

$$\begin{aligned}\tilde{Y} &= XW_q + (XA_k)B_k \\ &= X(W_q + A_k B_k) \\ &= X(W_q + \widetilde{E}_q) \\ &\approx X(W_q + E_q) \\ &= XW\end{aligned}\quad (9)$$

where $X \in \mathbb{R}^{t \times m}$ and $\tilde{Y} \in \mathbb{R}^{t \times n}$ are the layer input and the approximated output, and t is the sequence length. We use b_l and b_h to denote the bitwidth of low-precision matrix (W_q) and high-precision matrices (X , A_k and B_k) respectively. A pair of b_l and b_h , *e.g.*, $(b_l, b_h) = (3, 8)$, means that we compensate the quantization error of 3-bit weight using two 8-bit low-rank matrices. We refer to this design of the inference flow as LQER.

At inference-time, LQER runs one low-precision but large matrix multiplication (XW_q) and two high-precision but small matrix multiplications (XA_k and $(XA_k)B_k$) in parallel to save memory and achieve a speedup. Given a low-precision quantization $q(\cdot)$, adjusting the rank k allows tuning the trade-off between the computational cost and the model accuracy. Specifically:

- In LLMs, $W \in \mathbb{R}^{m \times n}$ is usually a large matrix. For example, (m, n) is $(12288, 12288)$, $(12288, 49152)$, or $(49152, 12288)$ in OPT-175B. A low-precision W_q significantly reduces the memory footprint and XW_q is faster than XW .
- Two high-precision but small matrices $A_k \in \mathbb{R}^{m \times k}$ and $B_k \in \mathbb{R}^{k \times n}$ estimate the quantization error at the cost of minimal computation. For a token $\mathbf{x} \in \mathbb{R}^m$, the two matrix multiplies $(\mathbf{x}A_k)$ and $((\mathbf{x}A_k)B_k)$ only introduce $(m+n) \times k$ high-precision multiplies in total while the unquantized $\mathbf{x}W$ has $m \times n$ high-precision multiplies. For the FNN layers in OPT-175B, the newly introduced multiplications is around $\frac{(m+n) \times k}{m \times n} \approx 0.01 \times k\%$.

The ideal case is that a small $k \ll \min(m, n)$, *e.g.*, $k = 32$, would successfully recover the model’s accuracy/perplexity. However, our experiments reveal that the singular values of E_q decay slowly for most linear layers, requiring a sufficiently large k to recover the accuracy/perplexity. Figure 3 illustrates the perplexity of quantized W3A8 OPT-1.3B versus rank k . For LQER, a small $k \approx 64$ still falls short compared to the FP16 baseline. The following section then discusses how we can achieve a low k value by analytically scaling the error term.

B. L²QER: Shape Singular Value Distribution of Quantization Errors using Activation Statistics

Recent works have shown that partially preserving the weight precision according to activation magnitude recovers the model’s accuracy/perplexity. `LLM.int8()` decomposes an FP16 matrix multiply into one FP16 sub-matrix multiply

for large activation magnitudes and one 8-bit fixed-point sub-matrix multiply for the rest at runtime. AWQ also presents an experiment that effectively recovers accuracy by preserving the 1% salient weights corresponding to large activation magnitudes in FP16, and quantizing other weights to 4-bit grouped fixed-point.

Motivated by this phenomenon, we propose a novel quantization error reconstruction method, named L²QER, that scales the quantization error matrix E_q before applying SVD and undo the scaling in low-rank matrices. We first left-multiply E_q with a diagonal matrix $S = \text{diag}(s_1, s_2, \dots, s_m)$ to scale i -th row of E_q by a distinct scalar s_i , then apply SVD to the scaled matrix SE_q :

$$SE_q = U' \Sigma' V'^T \approx U'_k \Sigma'_k V'^T_k \quad (10)$$

where S is calibrated from the pre-training data. To calculate s_i , we first average the i -th channel magnitudes across all the tokens in each calibration sample, then find the maximum average value among all samples. A detailed calculation of S is in Section A. The calibration requires no training.

The intuition behind the scaling is that the quantization error corresponds to large activation magnitudes, *i.e.*, the salient weights identified by corresponding activation magnitudes, should be more precisely approximated. Hence, we scale up these quantization errors before SVD.

High precision A'_k and B'_k are employed to cancel out S and reconstruct E_q :

$$\begin{cases} A'_k = S^{-1} U'_k \\ B'_k = \Sigma'_k V'^T_k \end{cases} \quad (11)$$

where S^{-1} is the inverse of the diagonal matrix S . S^{-1} always exists in practice since no diagonal elements in S is zero (no channels in LLM activations are always zero). Now we approximate the linear layer similarly to LQER:

$$\begin{aligned}\tilde{Y} &= XW_q + (XA'_k)B'_k \\ &= XW_q + (XS^{-1}U'_k)(\Sigma'_k V'^T_k) \\ &= X \left(W_q + S^{-1} \widetilde{(SE_q)}_k \right) \\ &\approx XW\end{aligned}\quad (12)$$

where \tilde{Y} and $\widetilde{(SE_q)}_k = U'_k \Sigma'_k V'^T_k$ are the approximated Y and the approximated (SE_q) of rank k . Note that the term $\widetilde{E}_q := S^{-1} \widetilde{(SE_q)}_k$ is the approximated quantization error.

As shown in Figure 1a, S drives the singular value distribution to decay faster than LQER with large singular values concentrating in the first few components, and the scaling is counteracted by S^{-1} in A'_k ; therefore, L²QER tends to recover more model capability than LQER. In Figure 3, L²QER recovers the perplexity close to FP16 baseline at a very small $k \approx 64$. In Section IV-C, we will show that L²QER achieves nearly lossless W4A6 LLM PTQ results comparable to state-of-the-art W6A6/W4A16 methods but with higher hardware efficiency.

TABLE II: Perplexity (\downarrow) of plain MXINT, LQER, and L²QER on OPT-1.3B and LLaMA-7B. We apply plain MXINT quantization, LQER, and L²QER to OPT-1.3B and LLaMA-7B in the same W4A8 setup. The decreasing perplexity proves the effectiveness of the quantization error reconstruction in LQER, and activation-induced scale matrix S in L²QER.

	MXINT	LQER	L ² QER	FP16
OPT-1.3B	16.42	15.28	15.02	14.63
Δ PPL (\downarrow)	+1.78	+0.65	+0.39	-
LLaMA-7B	6.17	6.06	5.89	5.67
Δ PPL (\downarrow)	+0.50	+0.39	+0.22	-

IV. EXPERIMENTS

A. Experimental Setup

a) Quantization: We use MXINT as the number format of LQER if not specified. In Section IV-C, we use W4A8 L²QER with $k = 32$ to compare with both 4-bit w -only and 4-/6-/8-bit $w&a$ quantization methods. In Section IV-D, we use W2A8 L²QER with $k = 256$ to compare with 2-bit w -only quantization methods. In both subsections, MXINT activation matrices have 8-bit shared exponents to accommodate activation outliers, while weight matrices and low-rank matrices have 4-bit shared exponents. The block size of MXINT is the default [1, 16] in the original paper [28] for X_q ([16, 1] for W_q , A_k , and B_k).

b) Models and Baselines: We benchmarked our methods on the OPT family [26], the LLaMA family (including LLaMA [38], LLaMA-2 [39], Vicuna-v1.5 [40]), and Mistral [41]. These are the representative or state-of-the-art model open-sourced for research across various model sizes and architectures. We compare our methods with FP16 model, LLM.int4()³, GPTQ, AWQ, AQAS, OmniQuant⁴, and QuiP. The later two have variants optimized for extremely low-precision quantization. We take the reported WikiText2 perplexity or downstream task accuracy from the original papers if available.

c) Evaluation: We report the perplexity on WikiText-2 [42] and the accuracy on ARC (easy) [43], ARC (challenge) [43], LAMBADA [44], PIQA [45], OpenBookQA [46], and BoolQ [47] using the lm-eval-harness evaluation flow [48]. Ideally a calibration dataset should be sampled from the pretraining dataset to calculate the activation-induced scale matrix S . However, none of the LLMs mentioned above open-sourced their pretraining datasets. We create a subset of SlimPajama [49] with Wikipedia texts excluded as the calibration dataset. This calibration dataset contains only 32 samples of 2048 tokens. As mentioned previously in Section III-B, this calibration simply profiles values without having any training. We also report the weight average bitwidth for mem-

³LLM.int4() denotes the 4-bit version of LLM.int8() open-sourced in bitsandbytes.

⁴We take W6A6 OmniQuant as an weight-activation quantization baseline, and W2A16 as a 2-bit weight-only quantization baseline.

ory efficiency and estimate the circuit area for the hardware cost. Circuit area is estimated with the number of Look Up Tables (LUTs) of the processing engines (PEs) if implemented on FPGAs, which is also approximately proportional to the number of gates if implemented as ASICs. We have faithfully implemented these arithmetic cores and inputted them into FPGA synthesis flows, obtaining results for circuit area. This is because MXINT is a newly release arithmetic standard [33]. Section D provides the detailed circuit area estimation.

B. LQER and L²QER

We first focus on comparing variants of LQER in Table II. We evaluate the variants in a W4A8 $w&a$ quantization setup on both OPT-1.3B and LLaMA-7B. We show the results of plain MXINT, LQER, and L²QER, where plain MXINT means the whole network is simply MXINT quantized without any special treatments.

Table II indicates that a plain W4A8 MXINT quantization leads to substantial performance degradation (Δ PPL = +1.78 on OPT-1.3B). LQER verifies that reconstructing the quantization error of weight helps to recover the model performance. Activation-induced S in L²QER further pushes the performance of LQER to be even closer to the FP16 baseline. In the following sections, we then mainly focus on presenting L²QER results.

C. Comparing with Existing Quantization Methods

We present the perplexity (\downarrow), the average increased perplexity over models (Δ PPL (\downarrow)), average weight bitwidth, and circuit area (\downarrow) of L²QER and existing w -only/ $w&a$ methods in Table III. Then we exclude the methods with obvious performance degradation and evaluate the average downstream task performance in Table IV. We additionally include a fixed-point version of L²QER as a baseline. Best results in each setup are marked in **bold** and second best results are underlined.

a) WikiText-2: In the w -only quantization setup, L²QER-INT achieves a significantly better perplexity when compared to GPTQ and is on par with AWQ (both only around 0.1 higher than FP16), while has a substantially smaller hardware cost (circuit area). In the $w&a$ setup, L²QER-MXINT has a perplexity around 0.15 higher than FP16 when it is W4A8. L²QER-MXINT outperforms state-of-the-art sub-8-bit methods by a significant margin. The perplexity of L²QER is around 0.05 higher than OmniQuant on the OPT family, but consistently outperforms OmniQuant on LLaMA family. Note that OmniQuant was trained on WikiText2 for 20 epochs [15], but L²QER only profiles the activation magnitudes using 32 samples from a calibration dataset with Wikipedia texts excluded. L²QER is also significantly smaller in terms of circuit area.

b) Downstream task accuracy: We conduct a thorough evaluation on downstream tasks, including ARC (easy), ARC (challenge), LAMBADA, PIQA, OpenBookQA and BoolQ and report the results in Table IV. The average accuracy of

TABLE III: A comparison of perplexity(\downarrow) on WikiText-2. Best results are marked in **bold**, and second best results are underlined in $w\&a$ setup. In a w -only setup, L²QER-INT outperforms GPTQ and is on par with AWQ, while offering substantially lower hardware costs. In a $w\&a$ setup, L²QER-MXINT outperforms all other competitors both in terms of perplexity and hardware efficiency. * means LLM.int4() casts the weight sub-matrices corresponding to activation outliers to 4-bit fixed-point before computation and cast them back to FP16 after, thus the weight formats in memory is FP16. † means OmniQuant and AQAS use per-channel and per-token scaled quantization. ‡ means LLaMA-2 results were not available in [12] and the author has not open-sourced AQAS code.

Q Setup	Method	Q Config	OPT			LLaMA			LLaMA-2		Avg. Δ PPL (\downarrow)	Avg. w bits	Circuit area (\downarrow)
			6.7B	13B	30B	7B	13B	33B	7B	13B			
-	FP16	-	10.86	10.13	9.56	5.67	5.10	4.10	5.48	4.90	-	16	1 \times
w -only	GPTQ	INT4, g128	11.39	10.31	9.63	6.12	5.21	4.24	5.69	4.98	0.22	4.1	13.99 \times
	AWQ	INT4, g128	10.93	10.21	9.59	5.78	5.20	4.22	5.61	4.98	0.09	4.1	13.99 \times
	L ² QER-INT	INT4, g128	10.99	10.24	9.57	5.89	5.20	4.24	5.58	4.96	0.11	4.3	1.34 \times
$w\&a$	LLM.int4()	$\tau = 6.0$	11.23	10.39	10.01	6.05	5.31	4.33	5.77	5.06	0.29	16*	21.23 \times
	OmniQuant †	W6A6, per-c/t	10.96	10.21	9.62	5.96	5.28	4.38	5.87	5.14	0.20	6.0	0.39 \times
	AQAS †	W4A8, per-c/t	13.42	12.19	11.08	6.69	5.81	5.14	-‡	-‡	1.45	4.0	0.45 \times
	L ² QER-INT	W4A8, g128	11.10	10.38	9.72	6.09	5.31	4.35	5.85	5.10	0.25	<u>4.1</u>	<u>0.33</u> \times
	L ² QER-MXINT	W4A6	11.03	10.32	9.72	<u>5.92</u>	<u>5.24</u>	<u>4.28</u>	<u>5.73</u>	<u>5.05</u>	<u>0.18</u>	4.3	0.23 \times
	L ² QER-MXINT	W4A8	<u>11.00</u>	<u>10.27</u>	<u>9.69</u>	5.89	5.21	4.25	5.69	5.02	0.15	4.3	<u>0.33</u> \times

TABLE IV: A comparison of downstream task accuracy (\uparrow), averaged across six downstream tasks. **Bold** text indicates the best results, while underscore denotes the second-best. L²QER achieves the best accuracy among all LLaMA models, and nearly lossless (around 0.3% drop) compared to the FP16 baseline. * means the results are not available in the original GPTQ paper, and we did not find open-source implementations and/or model checkpoints to run evaluation. † means the results of OPT and LLaMA-2 are not reported in the original OmniQuant paper. For LLaMA-1, LAMBADA and OpenbookQA are not included in OmniQuant either, thus we replace the results of these two tasks with FP16 results as an estimated upper limit of OmniQuant. OmniQuant-r is the results we replicated using the official implementation⁵ and checkpoints⁶.

Method	Q Config	OPT			LLaMA			LLaMA-2		Avg. Δ Accu. (\uparrow)
		6.7B	13B	30B	7B	13B	33B	7B	13B	
FP16	-	55.6%	56.2%	59.1%	63.2%	65.0%	68.4%	63.5%	66.5%	-
GPTQ	INT4, g128	55.4%	<u>56.4%</u>	-*	60.8%	64.7%	66.7%	62.2%	<u>65.9%</u>	-0.9%
AWQ	INT4, g128	<u>55.3%</u>	<u>56.4%</u>	58.9%	62.5%	<u>64.8%</u>	68.0%	62.9%	<u>65.9%</u>	-0.4%
LLM.int4()	$\tau = 6.0$	55.4%	55.9%	58.0%	62.2%	64.6%	67.7%	62.6%	65.8%	-0.7%
OmniQuant†	W6A6, per-c/t	-	-	-	58.4%	59.2%	61.0%	-	-	-6.0%
OmniQuant-r†	W6A6, per-c/t	55.4%	56.1%	<u>58.6%</u>	47.0%	48.2%	49.9%	47.2%	49.4%	-11.0%
L ² QER-INT	W4A8, g128	54.1%	56.2%	57.7%	61.7%	64.4%	67.4%	62.2%	<u>65.9%</u>	-1.0%
L ² QER-MXINT	W4A6	54.7%	56.2%	58.5%	<u>62.7%</u>	64.9%	<u>67.8%</u>	<u>63.0%</u>	65.8%	-0.5%
L ² QER-MXINT	W4A8	55.1%	56.5%	58.4%	63.0%	<u>64.8%</u>	68.0%	63.1%	66.1%	-0.3%

TABLE V: 2-bit quantization perplexity (\downarrow) on WikiText2. OmniQuant and QuiP#⁷ are two state-of-the-art methods for extremely low-precision LLM quantization. We found 2-bit quantization is still challenging for existing methods.

Q Setup	Method	Q Config	7B	13B
-	FP16	-	5.67	5.10
w -only	AWQ	INT2 g128	2.6e5	2.8e5
	QuiP#	INT2 g128	<u>10.97</u>	<u>8.43</u>
	OmniQuant	INT2 g128	12.97	10.36
$w\&a$	L ² QER	$k = 256$	10.30	8.42

L²QER on the six downstream tasks is better than other quantization methods on LLaMA models, and nearly lossless (around

0.3% drop) compared to the FP16 baseline. We reproduced the WikiText2 perplexity reported in OmniQuant paper [15] using the official implementation⁵ and checkpoints⁶, but failed to reproduce their downstream accuracy performance on LLaMA models. We refer to this mismatched OmniQuant results as OmniQuant-r in Table IV. We attribute the inconsistent behaviour of OmniQuant to its iterative quantization parameter training on WikiText2, which is further discussed in Section C. Nevertheless, our method has demonstrated substantially better downstream task capabilities, with a much lower hardware cost (circuit area in Table III). A detailed discussion about hardware cost is in Section D. A complete table including the accuracy

⁵<https://github.com/OpenGVLab/OmniQuant>

⁶<https://huggingface.co/ChenMnZ/OmniQuant/tree/main>

of each individual task is in Section E.

c) Optimization cost: The optimization of LQER is also efficient. The calibration and quantization of LLaMA-33B takes around 1.2 hour in total on a single NVIDIA A100 GPU. In contrast, OmniQuant takes 7.3 hours to optimize the quantization parameters for LLaMA-33B. Furthermore, the optimization of LQER can be fully parallelized to be faster, since there is no dependency between the quantization of each linear layer such as fusing the scale matrices to preceding layers in SmoothQuant or knowledge distillation in LLM-QAT [50].

D. 2-bit Quantization

To explore the limit of L²QER, we evaluate L²QER in the 2-bit quantization setup. Table V compares L²QER with OmniQuant and QuiP#⁷, which are both recent works optimized for extremely low-precision LLM quantization. We observe that 2-bit quantization is challenging for existing methods including L²QER. These methods perform inconsistently with model sizes and families (Table XVII in Section E). Unlike a simple rank $k = 32$ for W4A8 quantization, L²QER requires a larger k for 2-bit quantization.

E. L²QER with Different Model Families

To fully evaluate the adaptiveness of L²QER across model families, we have also conducted experiments to evaluate its effectiveness on Vicuna and Mistral. The results of Vicuna-v1.5-7B/13B and Mistral-7B are included in Section E. These results reveal a pattern consistent with other models, indicating that L²QER is agnostic to various LLM families.

V. CONCLUSION

In this work, we propose a novel LLM post-training quantization framework, LQER, which judiciously combine quantization and low-rank approximation to recover model capability. We then further propose L²QER, which leverages an activation-induced scale matrix to shape the singular values of quantization error towards a desirable distribution that can be accurately approximated. L²QER achieves nearly-losses perplexity (around 0.15 higher than FP16) and an average accuracy drop of only around 0.3% on six different downstream tasks. The regular computation pattern of LQER ensures a higher hardware efficiency than existing methods and takes 67% smaller circuit area than FP16.

VI. BROADER IMPACTS

This paper presents work whose goal is to advance the field of Machine Learning. There are many potential societal consequences of our work, none which we feel must be specifically highlighted here.

⁷QuiP# is an improved version of QuiP released by the same research group: <https://github.com/Cornell-RelaxML/quip-sharp>

REFERENCES

- [1] T. Brown, B. Mann, N. Ryder, M. Subbiah, J. D. Kaplan, P. Dhariwal, A. Neelakantan, P. Shyam, G. Sastry, A. Askell *et al.*, “Language models are few-shot learners,” *Advances in neural information processing systems*, vol. 33, pp. 1877–1901, 2020.
- [2] B. Workshop, T. L. Scao, A. Fan, C. Akiki, E. Pavlick, S. Ilić, D. Hesslow, R. Castagné, A. S. Luccioni, F. Yvon *et al.*, “Bloom: A 176b-parameter open-access multilingual language model,” *arXiv preprint arXiv:2211.05100*, 2022.
- [3] A. S. Luccioni, S. Viguier, and A.-L. Ligozat, “Estimating the carbon footprint of bloom, a 176b parameter language model,” *Journal of Machine Learning Research*, vol. 24, no. 253, pp. 1–15, 2023.
- [4] J. Hoffmann, S. Borgeaud, A. Mensch, E. Buchatskaya, T. Cai, E. Rutherford, D. d. L. Casas, L. A. Hendricks, J. Welbl, A. Clark *et al.*, “Training compute-optimal large language models,” *arXiv preprint arXiv:2203.15556*, 2022.
- [5] M. Nagel, M. Fournarakis, R. A. Amjad, Y. Bondarenko, M. Van Baalen, and T. Blankevoort, “A white paper on neural network quantization,” *arXiv preprint arXiv:2106.08295*, 2021.
- [6] X. Wei, Y. Zhang, X. Zhang, R. Gong, S. Zhang, Q. Zhang, F. Yu, and X. Liu, “Outlier suppression: Pushing the limit of low-bit transformer language models,” *Advances in Neural Information Processing Systems*, vol. 35, pp. 17402–17414, 2022.
- [7] Y. Bondarenko, M. Nagel, and T. Blankevoort, “Understanding and overcoming the challenges of efficient transformer quantization,” *arXiv preprint arXiv:2109.12948*, 2021.
- [8] H. Tang, Y. Sun, D. Wu, K. Liu, J. Zhu, and Z. Kang, “Easyquant: An efficient data-free quantization algorithm for llms,” in *Proceedings of the 2023 Conference on Empirical Methods in Natural Language Processing*, 2023, pp. 9119–9128.
- [9] T. Dettmers, M. Lewis, Y. Belkada, and L. Zettlemoyer, “Llm.int8(): 8-bit matrix multiplication for transformers at scale,” *arXiv preprint arXiv:2208.07339*, 2022.
- [10] E. Frantar, S. Ashkboos, T. Hoefler, and D. Alistarh, “Gptq: Accurate post-training quantization for generative pre-trained transformers,” *arXiv preprint arXiv:2210.17323*, 2022.
- [11] G. Xiao, J. Lin, M. Seznec, H. Wu, J. Demouth, and S. Han, “Smoothquant: Accurate and efficient post-training quantization for large language models,” in *International Conference on Machine Learning*. PMLR, 2023, pp. 38087–38099.
- [12] J. Lee, M. Kim, S. Baek, S. J. Hwang, W. Sung, and J. Choi, “Enhancing computation efficiency in large language models through weight and activation quantization,” *arXiv preprint arXiv:2311.05161*, 2023.
- [13] X. Wei, Y. Zhang, Y. Li, X. Zhang, R. Gong, J. Guo, and

- X. Liu, "Outlier suppression+: Accurate quantization of large language models by equivalent and optimal shifting and scaling," *arXiv preprint arXiv:2304.09145*, 2023.
- [14] Y. Bondarenko, M. Nagel, and T. Blankevoort, "Quantizable transformers: Removing outliers by helping attention heads do nothing," *arXiv preprint arXiv:2306.12929*, 2023.
- [15] W. Shao, M. Chen, Z. Zhang, P. Xu, L. Zhao, Z. Li, K. Zhang, P. Gao, Y. Qiao, and P. Luo, "OmniQuant: Omnidirectionally calibrated quantization for large language models," *arXiv preprint arXiv:2308.13137*, 2023.
- [16] L. Lin, "LLM-Tracker: OmniQuant," 2024. [Online]. Available: <https://llm-tracker.info/howto/OmniQuant>
- [17] J. Lin, J. Tang, H. Tang, S. Yang, X. Dang, and S. Han, "Awq: Activation-aware weight quantization for llm compression and acceleration," *arXiv preprint arXiv:2306.00978*, 2023.
- [18] C. Hansen, "Autoawq," <https://github.com/casper-hansen/AutoAWQ>, 2024.
- [19] T. Dettmers, R. Svirschevski, V. Egiastian, D. Kuznedelev, E. Frantar, S. Ashkboos, A. Borzunov, T. Hoefer, and D. Alistarh, "Spqr: A sparse-quantized representation for near-lossless llm weight compression," *arXiv preprint arXiv:2306.03078*, 2023.
- [20] J. H. Lee, J. Kim, S. J. Kwon, and D. Lee, "Flexround: Learnable rounding based on element-wise division for post-training quantization," *arXiv preprint arXiv:2306.00317*, 2023.
- [21] Y. Jeon, C. Lee, K. Park, and H.-y. Kim, "A frustratingly easy post-training quantization scheme for llms," in *Proceedings of the 2023 Conference on Empirical Methods in Natural Language Processing*, 2023, pp. 14446–14461.
- [22] J. Chee, Y. Cai, V. Kuleshov, and C. De Sa, "Quip: 2-bit quantization of large language models with guarantees," *arXiv preprint arXiv:2307.13304*, 2023.
- [23] Y. Luo, Y. Gao, Z. Zhang, J. Fan, H. Zhang, and M. Xu, "Long-range zero-shot generative deep network quantization," *Neural Networks*, vol. 166, pp. 683–691, 2023.
- [24] B. D. Rouhani, R. Zhao, A. More, M. Hall, A. Khodamoradi, S. Deng, D. Choudhary, M. Cornea, E. Dellinger, K. Denolf *et al.*, "Microscaling data formats for deep learning," *arXiv preprint arXiv:2310.10537*, 2023.
- [25] V. Marchenko and L. Pastur, "Distribution of eigenvalues for some sets of random matrices," *Mat. Sb*, vol. 72, pp. 507–536, 1967.
- [26] S. Zhang, S. Roller, N. Goyal, M. Artetxe, M. Chen, S. Chen, C. Dewan, M. Diab, X. Li, X. V. Lin *et al.*, "Opt: Open pre-trained transformer language models," *arXiv preprint arXiv:2205.01068*, 2022.
- [27] J. Liu, R. Gong, X. Wei, Z. Dong, J. Cai, and B. Zhuang, "Qllm: Accurate and efficient low-bitwidth quantization for large language models," *arXiv preprint arXiv:2310.08041*, 2023.
- [28] B. Darvish Rouhani, D. Lo, R. Zhao, M. Liu, J. Fowers, K. Ovtcharov, A. Vinogradsky, S. Massengill, L. Yang, R. Bittner *et al.*, "Pushing the limits of narrow precision inferencing at cloud scale with microsoft floating point," *Advances in neural information processing systems*, vol. 33, pp. 10271–10281, 2020.
- [29] S. Fox, S. Rasoulinezhad, J. Faraone, P. Leong *et al.*, "A block minifloat representation for training deep neural networks," in *International Conference on Learning Representations*, 2020.
- [30] S. Q. Zhang, B. McDanel, and H. Kung, "Fast: Dnn training under variable precision block floating point with stochastic rounding," in *2022 IEEE International Symposium on High-Performance Computer Architecture (HPCA)*. IEEE, 2022, pp. 846–860.
- [31] M. Drumond, T. Lin, M. Jaggi, and B. Falsafi, "Training dnns with hybrid block floating point," *Advances in Neural Information Processing Systems*, vol. 31, 2018.
- [32] B. Rouhani, R. Zhao, V. Elango, R. Shafipour, M. Hall, M. Mesmakhosroshahi, A. More, L. Melnick, M. Golub, G. Varatkar *et al.*, "Shared microexponents: A little shifting goes a long way," *arXiv preprint arXiv:2302.08007*, 2023.
- [33] P. Micikevicius, S. Oberman, P. Dubey, M. Cornea, A. Rodriguez, I. Bratt, R. Grisenthwaite, N. Jouppi, C. Chou, A. Huffman, M. Schulte, R. Wittig, D. Jani, and S. Deng, "Ocp 8-bit floating point specification (ofp8)," 2023. [Online]. Available: <https://www.opencompute.org/documents/ocp-microscaling-formats-mx-v1-0-spec-final-pdf>
- [34] C. Zhang, J. Cheng, I. Shumailov, G. Constantinides, and Y. Zhao, "Revisiting block-based quantisation: What is important for sub-8-bit LLM inference?" in *Proceedings of the 2023 Conference on Empirical Methods in Natural Language Processing*, H. Bouamor, J. Pino, and K. Bali, Eds. Singapore: Association for Computational Linguistics, Dec. 2023, pp. 9988–10006. [Online]. Available: <https://aclanthology.org/2023.emnlp-main.617>
- [35] E. J. Hu, Y. Shen, P. Wallis, Z. Allen-Zhu, Y. Li, S. Wang, L. Wang, and W. Chen, "Lora: Low-rank adaptation of large language models," *arXiv preprint arXiv:2106.09685*, 2021.
- [36] T. Dettmers, A. Pagnoni, A. Holtzman, and L. Zettlemoyer, "Qlora: Efficient finetuning of quantized llms," *arXiv preprint arXiv:2305.14314*, 2023.
- [37] Y. Li, Y. Yu, C. Liang, P. He, N. Karampatziakis, W. Chen, and T. Zhao, "Loftq: Lora-fine-tuning-aware quantization for large language models," *arXiv preprint arXiv:2310.08659*, 2023.
- [38] H. Touvron, T. Lavril, G. Izacard, X. Martinet, M.-A. Lachaux, T. Lacroix, B. Rozière, N. Goyal, E. Hambro, F. Azhar *et al.*, "Llama: Open and efficient foundation language models," *arXiv preprint arXiv:2302.13971*, 2023.
- [39] H. Touvron, L. Martin, K. Stone, P. Albert, A. Almahairi, Y. Babaei, N. Bashlykov, S. Batra, P. Bhargava, S. Bhos-

- ale *et al.*, “Llama 2: Open foundation and fine-tuned chat models,” *arXiv preprint arXiv:2307.09288*, 2023.
- [40] L. Zheng, W.-L. Chiang, Y. Sheng, S. Zhuang, Z. Wu, Y. Zhuang, Z. Lin, Z. Li, D. Li, E. Xing *et al.*, “Judging llm-as-a-judge with mt-bench and chatbot arena,” *arXiv preprint arXiv:2306.05685*, 2023.
- [41] A. Q. Jiang, A. Sablayrolles, A. Mensch, C. Bamford, D. S. Chaplot, D. d. l. Casas, F. Bressand, G. Lengyel, G. Lample, L. Saulnier *et al.*, “Mistral 7b,” *arXiv preprint arXiv:2310.06825*, 2023.
- [42] S. Merity, C. Xiong, J. Bradbury, and R. Socher, “Pointer sentinel mixture models,” 2016.
- [43] P. Clark, I. Cowhey, O. Etzioni, T. Khot, A. Sabharwal, C. Schoenick, and O. Tafjord, “Think you have solved question answering? try arc, the ai2 reasoning challenge,” *arXiv:1803.05457v1*, 2018.
- [44] D. Paperno, G. Kruszewski, A. Lazaridou, Q. N. Pham, R. Bernardi, S. Pezzelle, M. Baroni, G. Boleda, and R. Fernández, “The lambada dataset: Word prediction requiring a broad discourse context,” *arXiv preprint arXiv:1606.06031*, 2016.
- [45] Y. Bisk, R. Zellers, R. L. Bras, J. Gao, and Y. Choi, “Piqa: Reasoning about physical commonsense in natural language,” in *Thirty-Fourth AAAI Conference on Artificial Intelligence*, 2020.
- [46] T. Mihaylov, P. Clark, T. Khot, and A. Sabharwal, “Can a suit of armor conduct electricity? a new dataset for open book question answering,” in *EMNLP*, 2018.
- [47] C. Clark, K. Lee, M.-W. Chang, T. Kwiatkowski, M. Collins, and K. Toutanova, “Boolq: Exploring the surprising difficulty of natural yes/no questions,” *arXiv preprint arXiv:1905.10044*, 2019.
- [48] L. Gao, J. Tow, B. Abbasi, S. Biderman, S. Black, A. DiPofi, C. Foster, L. Golding, J. Hsu, A. Le Noac’h, H. Li, K. McDonell, N. Muennighoff, C. Ociepa, J. Phang, L. Reynolds, H. Schoelkopf, A. Skowron, L. Sutawika, E. Tang, A. Thite, B. Wang, K. Wang, and A. Zou, “A framework for few-shot language model evaluation,” 12 2023. [Online]. Available: <https://zenodo.org/records/10256836>
- [49] D. Soboleva, F. Al-Khateeb, R. Myers, J. R. Steeves, J. Hestness, and N. Dey, “SlimPajama: A 627B token cleaned and deduplicated version of RedPajama,” <https://www.cerebras.net/blog/slimpajama-a-627b-token-cleaned-and-deduplicated-version-of-redpajama>, 2023. [Online]. Available: <https://huggingface.co/datasets/cerebras/SlimPajama-627B>
- [50] Z. Liu, B. Oguz, C. Zhao, E. Chang, P. Stock, Y. Mehdad, Y. Shi, R. Krishnamoorthi, and V. Chandra, “Llm-qat: Data-free quantization aware training for large language models,” *arXiv preprint arXiv:2305.17888*, 2023.

APPENDIX A DATA CALIBRATION

Given a calibration dataset containing N samples, $\{X_i \mid i = 1, 2, \dots, N\}$, we first profile the activation magnitude for each channel,

$$\begin{aligned} \mathbf{a}_i &= \text{mean}(|X_i|, \text{axis} = 0), \\ \bar{\mathbf{a}} &= \max\left(\begin{bmatrix} \mathbf{a}_1 \\ \vdots \\ \mathbf{a}_N \end{bmatrix}, \text{axis} = 0\right), \end{aligned} \quad (13)$$

where $|\cdot|$ calculates the element-wise absolute value and $\bar{\mathbf{a}} = [a_1, a_2, \dots, a_m]$ is a row vector of maximum channel magnitudes across samples. We normalize $\bar{\mathbf{a}}$ to get the diagonal matrix S :

$$s_i = \frac{a_i}{\sqrt{\min(\bar{\mathbf{a}}) \times \max(\bar{\mathbf{a}})}}, \quad (14)$$

Equation (13) and Equation (14) are empirical implementation based on [17]. We leave the exploration of an analytical derivation of S as future work.

APPENDIX B SINGULAR VALUE DISTRIBUTIONS OF LQER AND L²QER

Here we present a few representative singular value distributions of quantization errors for LLaMA-7B in Figure 4. We observe that the singular values of most layers are driven towards desirable distributions by L²QER. Most O projection layers and a few layers at the beginning or the end of the model tend to have an Eq distribution decaying slowly.

We also visualize the approximation error of LQER and LQER versus layer index in Figure 5. The approximation error is measured as:

$$e_a = \frac{1}{mn} \sum_{i=1}^m \sum_{j=1}^n (|E_q - \tilde{E}_q|_{i,j}) \quad (15)$$

where $|\cdot|$ calculate the element-wise absolute value. L²QER reconstructs the quantization error more accurate than LQER on most layers, while LQER better reconstruct the K, Q, and V projection layers at the 1st, 3rd, and 4th transformer layers.

APPENDIX C INCONSISTANT PERFORMANCE OF OMNIQUANT ON WIKITEXT2 AND DOWNSTREAM TASKS

OmniQuant is one of the state-of-the-art LLM post-training-quantization methods we compared in this work. Thanks for the official open-sourced implementation and quantization parameter checkpoints, we performed extensive experiments to compare OmniQuant to LQER. We successfully reproduce the perplexity and downstream task accuracy of OPT-family. However, the LLaMA models quantized by OmniQuant have obvious performance degradation on downstream tasks, around 18.9% lower than FP16 baselines on average.

We attribute this performance degradation to the iterative gradient-base training on WikiText2 in OmniQuant. As stated in [15], OmniQuant optimizes the quantization parameter (shifts and scales) by training on WikiText2 samples for 20

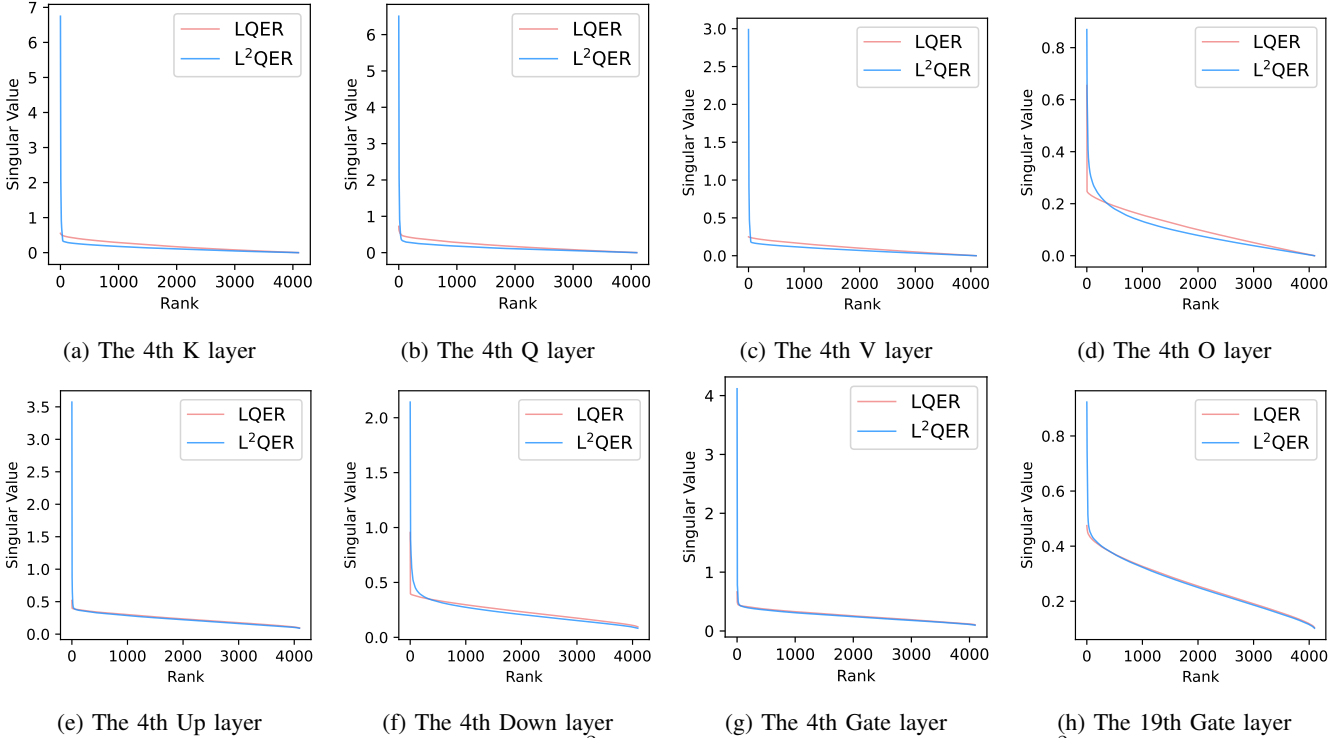


Fig. 4: The singular value distributions of LQER and L^2 QER. We find that the shaping effect of L^2 QER are obvious on most layers in LLaMA. Most O projection layers and several layers at the beginning or the end of the model tend to have an E_q distribution decaying slowly (See Figure 4d and Figure 4h).

epochs (40 epochs for W2A16). This training requires tuning the hyper-parameters such as number of training samples, learning rates and total number of epochs, which may cause overfitting or underfitting if not tuned properly. Both cases can be the reason for performance degradation.

APPENDIX D ESTIMATE HARDWARE COST

We estimate the memory efficiency with average bitwidth. The average bitwidth of per-channel scaled quantization is considered as the average bits of an FP16 scalar and m fixed-point numbers, where m is the input hidden size. The average bitwidth of $MXINT$ is averaged across one shared exponent and B mantissas, where B is the block size. For LQER/ L^2 QER, this is averaged across the low-precision W_q and the high-precision A_k and B_k . The average weight bitwidth of L^2 QER in memory is 0.2 higher than GPTQ and AWQ, which is mainly contributed by the two low-rank matrices A_k and B_k . L^2 QER outperforms existing nearly lossless methods in terms of circuit area, because it is free from expensive element-wise dequantization (GPTQ and AWQ), or scatter/gather operations (`LLM.int4()`) at runtime.

We estimate the hardware cost with circuit area. We mapped the algorithms of these approaches onto custom hardware accelerators on FPGAs. To ensure fairness, these hardware accelerators have the same throughput of 16 multiply-accumulate (MAC) operations per clock cycle when computing a linear

operation of the same matrix sizes. We then measure the circuit area in terms of LUTs and Digital Signal Processing blocks (DSPs) on the FPGA, where a DSP is treated as 100 LUTs. The area results were measured from the Place & Route report in Xilinx Vivado 2023.1. The FPGA family that we used for all the experiments is Xilinx Alveo U250.

APPENDIX E MORE EVALUATION RESULTS

We present the complete results of each specific downstream tasks in Tables VI to XIII. We also tested L^2 QER on Vicuna-7b/13b and Mistral-7b-v0.1 in Tables XIV to XVI.

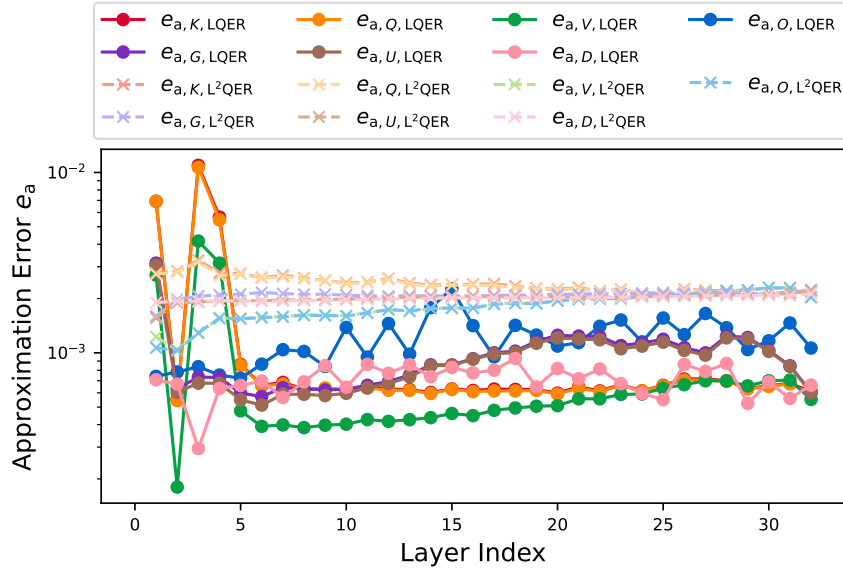


Fig. 5: Approximation error of LQER and L^2 QER across decoder layers in LLaMA-7B. L^2 QER produces smaller approximation errors on most of the linear layers in transformer-based LLMs. However, there are a few layers better reconstructed by LQER, such as the key, value, output project layers in 1st, 3rd, and 4th decoder layer. The derivation of S worths further exploration.

TABLE VI: OPT-6.7B

Method	WikiText2	ARC (easy)	ARC (challenge)	LAMBADA	PIQA	BOOLQ	OpenbookQA	Avg. Accuracy
FP16	10.86	65.6%	30.5%	67.7%	76.3%	66.1%	27.6%	55.6%
GPTQ	10.95	65.6%	31.1%	68.5%	76.2%	65.2%	26.2%	55.4%
AWQ	10.93	65.3%	30.5%	67.4%	76.6%	65.2%	26.6%	55.3%
LLM.int4()	11.23	65.3%	30.5%	67.4%	76.6%	65.2%	26.6%	55.3%
OmniQuant (W6A6)	10.96	65.4%	30.9%	66.9%	76.0%	66.2%	26.8%	55.4%
LQER-INT (W4A8)	11.10	63.8%	29.6%	65.7%	75.6%	63.1%	26.8%	54.1%
LQER-MXINT (W4A6)	11.03	65.4%	30.5%	65.6%	75.4%	64.0%	27.6%	54.7%
LQER-MXINT (W4A8)	11.00	65.2%	30.4%	66.3%	75.5%	65.3%	27.6%	55.0%

TABLE VII: OPT-13B

Method	WikiText2	ARC (easy)	ARC (challenge)	LAMBADA	PIQA	BOOLQ	OpenbookQA	Avg. Accuracy
FP16	10.13	67.1%	32.9%	68.6%	76.0%	65.8%	27.0%	56.2%
GPTQ	10.31	67.5%	32.8%	68.8%	76.1%	65.9%	27.2%	56.4%
AWQ	10.21	66.8%	33.3%	68.2%	75.6%	66.5%	28.0%	56.4%
LLM.int4()	10.39	66.2%	33.6%	67.8%	76.2%	67.3%	24.2%	55.9%
OmniQuant (W6A6)	10.96	67.1%	33.1%	68.4%	76.2%	65.3%	26.4%	56.1%
LQER-INT (W4A8)	10.38	66.5%	33.2%	67.5%	75.5%	67.9%	26.4%	56.2%
LQER-MXINT (W4A6)	10.32	67.2%	32.2%	67.9%	75.7%	68.3%	25.8%	56.2%
LQER-MXINT (W4A8)	10.27	67.4%	32.6%	68.4%	76.1%	68.3%	26.2%	56.5%

TABLE VIII: OPT-6.7B

Method	WikiText2	ARC (easy)	ARC (challenge)	LAMBADA	PIQA	BOOLQ	OpenbookQA	Avg. Accuracy
FP16	9.56	70.0%	34.6%	71.5%	77.6%	70.5%	30.2%	59.1%
GPTQ	9.63	62.2%	29.4%	74.9%	67.6%	69.1%	23.8%	54.5%
AWQ	9.59	69.7%	34.6%	71.6%	77.3%	70.4%	30.0%	58.9%
LLM.int4()	10.01	69.0%	32.8%	71.3%	76.9%	70.2%	27.8%	58.0%
OmniQuant (W6A6)	9.62	70.1%	34.2%	70.4%	77.3%	70.2%	29.6%	58.6%
LQER-INT (W4A8)	9.72							
LQER-MXINT (W4A6)	9.72	0.6990740741	0.3421501706	0.7050261983	0.7725788901	0.6923547401	0.298	58.5%
LQER-MXINT (W4A8)	9.67	69.4%	34.4%	70.4%	77.3%	69.5%	29.6%	58.4%

TABLE IX: llama-7B

Method	WikiText2	ARC (easy)	ARC (challenge)	LAMBADA	PIQA	BOOLQ	OpenbookQA	Avg. Accuracy
FP16	5.10	77.4%	46.4%	76.2%	79.1%	78.0%	33.2%	65.0%
GPTQ	5.21	76.9%	46.8%	75.0%	79.3%	76.4%	34.0%	64.7%
AWQ	5.20	77.2%	46.4%	75.6%	79.0%	77.8%	32.8%	64.8%
LLM.int4()	5.31	77.2%	46.0%	75.4%	78.9%	77.1%	32.8%	64.6%
OmniQuant (W6A6)	5.28	72.5%	42.9%	0.0%	78.2%	66.4%	29.0%	48.2%
LQER-INT (W4A8)	5.31	76.9%	45.9%	74.0%	78.7%	77.2%	33.6%	64.4%
LQER-MXINT (W4A6)	5.24	77.1%	46.2%	75.6%	79.2%	77.6%	33.6%	64.9%
LQER-MXINT (W4A8)	5.21	77.0%	46.3%	75.6%	79.6%	77.3%	33.2%	64.8%

TABLE X: LLaMA-13B

Method	WikiText2	ARC (easy)	ARC (challenge)	LAMBADA	PIQA	BOOLQ	OpenbookQA	Avg. Accuracy
FP16	5.67	75.4%	41.9%	73.5%	78.7%	75.1%	34.4%	63.2%
GPTQ	9.63	73.6%	40.4%	70.0%	77.7%	73.0%	30.0%	60.8%
AWQ	9.59	75.5%	41.1%	72.5%	78.6%	74.9%	32.2%	62.5%
LLM.int4()	10.01	74.6%	42.1%	70.3%	78.6%	74.8%	32.8%	62.2%
OmniQuant (W6A6)	9.62	66.4%	38.8%	0.0%	76.7%	72.8%	27.2%	47.0%
LQER-INT (W4A8)	6.09	73.9%	40.6%	73.4%	77.7%	74.0%	30.6%	61.7%
LQER-MXINT (W4A6)	5.92	74.8%	41.5%	73.4%	78.2%	75.2%	33.0%	62.7%
LQER-MXINT (W4A8)	5.89	74.9%	41.6%	73.3%	78.6%	76.1%	33.6%	63.0%

TABLE XI: LLaMA-30B

Method	WikiText2	ARC (easy)	ARC (challenge)	LAMBADA	PIQA	BOOLQ	OpenbookQA	Avg. Accuracy
FP16	4.10	80.4%	52.8%	77.6%	81.1%	82.7%	36.0%	68.4%
GPTQ	4.24	80.7%	50.2%	77.6%	80.5%	83.1%	35.8%	68.0%
AWQ	4.22	74.1%	46.0%	0.0%	79.5%	68.3%	31.4%	49.9%
LLM.int4()	4.33	79.0%	48.9%	75.8%	80.2%	82.4%	33.6%	66.7%
OmniQuant (W6A6)	4.38	74.1%	46.0%	0.0%	79.5%	68.3%	31.4%	49.9%
LQER-INT (W4A8)	4.35	80.1%	49.7%	77.0%	80.7%	81.5%	35.2%	67.4%
LQER-MXINT (W4A6)	4.28	80.1%	50.9%	77.4%	80.6%	82.4%	35.4%	67.8%
LQER-MXINT (W4A8)	4.25	80.0%	50.8%	77.6%	80.7%	82.5%	36.2%	68.0%

TABLE XII: LLaMA-2-7B

Method	WikiText2	ARC (easy)	ARC (challenge)	LAMBADA	PIQA	BOOLQ	OpenbookQA	Avg. Accuracy
FP16	5.48	76.3%	43.6%	73.9%	78.1%	77.7%	31.4%	63.5%
GPTQ	5.69	75.0%	42.2%	72.3%	77.4%	76.4%	30.0%	62.2%
AWQ	5.61	75.2%	43.3%	72.7%	77.6%	77.3%	31.4%	62.9%
LLM.int4()	5.77	75.1%	42.7%	71.9%	77.6%	76.2%	32.2%	62.6%
OmniQuant (W6A6)	5.87	67.3%	39.0%	0.0%	77.6%	69.9%	29.2%	47.2%
LQER-INT (W4A8)	5.85	74.7%	42.4%	71.6%	76.7%	76.1%	32.0%	62.2%
LQER-MXINT (W4A6)	5.73	75.1%	43.1%	73.6%	77.6%	76.2%	32.6%	63.0%
LQER-MXINT (W4A8)	5.69	75.3%	42.5%	73.7%	77.9%	76.3%	32.8%	63.1%

TABLE XIII: LLaMA-2-13B

Method	WikiText2	ARC (easy)	ARC (challenge)	LAMBADA	PIQA	BOOLQ	OpenbookQA	Avg. Accuracy
FP16	4.90	79.4%	48.3%	76.7%	79.1%	80.6%	35.0%	66.5%
GPTQ	5.06	78.6%	47.4%	76.4%	78.2%	80.8%	34.2%	65.9%
AWQ	4.98	78.9%	46.9%	76.2%	78.8%	80.1%	34.4%	65.9%
LLM.int4()	4.98	77.6%	47.0%	76.1%	78.9%	80.5%	34.8%	65.8%
OmniQuant (W6A6)	5.14	71.3%	43.8%	0.0%	78.6%	69.8%	33.0%	49.4%
LQER-INT (W4A8)	5.10	78.5%	47.1%	75.8%	78.6%	81.0%	34.4%	65.9%
LQER-MXINT (W4A6)	5.05	78.2%	46.4%	76.4%	78.3%	80.6%	34.8%	65.8%
LQER-MXINT (W4A8)	5.02	78.3%	47.0%	76.4%	78.8%	81.3%	34.6%	66.1%

TABLE XIV: Vicuna-7B-v1.5

Method	WikiText2	ARC (easy)	ARC (challenge)	LAMBADA	PIQA	BOOLQ	OpenbookQA	Avg. Accuracy
FP16	6.78	75.6%	43.3%	71.1%	77.3%	80.9%	33.0%	63.5%
GPTQ	7.07	75.4%	41.5%	69.4%	76.0%	81.3%	33.2%	62.8%
AWQ	7.00	75.0%	41.8%	70.0%	77.1%	81.5%	32.2%	62.9%
LLM.int4()	7.14	75.0%	42.6%	69.3%	76.3%	81.3%	34.2%	63.1%
LQER-MXINT (W4A8)	7.01	75.4%	42.2%	68.9%	77.1%	81.6%	33.0%	63.0%

TABLE XV: Vicuna-13B-v1.5

Method	WikiText2	ARC (easy)	ARC (challenge)	LAMBADA	PIQA	BOOLQ	OpenbookQA	Avg. Accuracy
FP16	5.92	78.7%	47.8%	73.4%	78.9%	85.2%	36.8%	66.8%
GPTQ	6.00	77.9%	46.4%	72.9%	78.1%	85.0%	36.8%	66.2%
AWQ	6.03	78.3%	48.4%	72.9%	78.3%	84.8%	36.8%	66.6%
LLM.int4()	6.09	77.5%	47.3%	73.0%	78.3%	85.2%	36.8%	66.4%
LQER-MXINT (W4A8)	6.04	78.5%	46.7%	72.7%	77.7%	85.0%	36.4%	66.2%

TABLE XVI: Mistral-7B

Method	WikiText2	ARC (easy)	ARC (challenge)	LAMBADA	PIQA	BOOLQ	OpenbookQA	Avg. Accuracy
FP16	6.47	82.7%	53.5%	70.7%	80.4%	86.2%	32.8%	67.7%
GPTQ	8.13	81.1%	55.8%	72.2%	80.9%	86.7%	36.0%	68.8%
AWQ	6.64	81.9%	53.8%	71.8%	80.7%	86.2%	37.4%	68.6%
LLM.int4()	6.66	81.2%	53.2%	70.6%	81.2%	86.4%	34.6%	67.9%
LQER-MXINT (W4A8)	6.71	81.7%	53.8%	71.2%	81.0%	86.5%	34.8%	68.2%

TABLE XVII: More 2-bit w -only results. These methods perform inconsistently with model sizes and families. Unlike a simple rank $k = 32$ for W4A8 quantization, L²QER requires a larger rank k for 2-bit quantization.

Method	OPT			LLaMA	
	125M	1.3B	2.7B	7B	13B
FP16	27.65	14.63	12.47	5.67	5.10
OmniQuant	<u>75.43</u>	23.95	18.13	12.97	10.36
Quip	347.40	41.64	2998.00	<u>10.97</u>	<u>8.43</u>
L ² QER	45.29	<u>29.82</u>	<u>23.76</u>	10.30	8.42